Reflection of Electromagnetic Waves on Moving Interfaces for Analyzing Shock Phenomenon in Solids

Benoit Rougier, Hervé Aubert, A Lefrançois, Yohan Barbarin, J. Luc, A. Osmont

Reflection of Electromagnetic Waves on Moving Interfaces for Analyzing Shock Phenomenon in Solids

B. Rougier[1,2], H. Aubert[2], A. Lefrançois[1], Y. Barbarin[1], J. Luc[1] and A. Osmont[1]

[1] CEA, CEA-Gramat, F-46500 Gramat, France

[2] LAAS-CNRS, Université de Toulouse, CNRS, INPT, 7 avenue du Colonel Roche, 31077 Toulouse, France

Abstract

A new closed-form expression is derived in this paper for computing the electromagnetic field reflected by two moving interfaces. The interfaces velocities and refractive index between interfaces are then derived from measurable frequencies and amplitudes embedded in the reflected electromagnetic field. As an application, the remote analysis of the shock wave phenomenon in solids is reported and shock wave descriptors are estimated. Based on the proposed approach, physical insights on published measurement results are reported. Two cases are investigated: one from the literature and one from new data on shock loading of PolyMethyl MethAcrylate.

1 Introduction

Electromagnetic waves allow the continuous and non-invasive analysis of shock wave phenomenon in radio-transparent solids. In a solid under intense mechanical loading, a shock wave is generated ([*Meyers*(1994)]). This wave propagates faster than the sound in the solid and modifies the mechanical and thermodynamical properties of the material. As a result, the mass density of the material changes. As the permittivity of material depends on this density (see *e.g.* [*Cox and Merz*(1958)]), the permittivity varies when a solid is subjected to a shock loading. Moreover, a shock wave changes the velocity of the material. This velocity is called the *particle velocity*. From the measurement of the shock wavefront velocity and the particle velocity, it is possible to derive the parameters of the linear relationship between the velocity of the shock wave and the particle velocity ([*Meyers*(1994)]). Radars ([*Anderson and Kelly*(1967)]) and radio-interferometers ([*Koch*(1969)]) can advantageously be used for probing materials under shock and exploring the physics behind the shock wave. [*Luther et al.*(1991)] and [*Luther and Warren*(1994)] reported the first application with a microwave (9 GHz) interferometer for deriving the particle and shock wavefront velocities in Teflon from two specific oscillations observed in the reflected electromagnetic signal: the higher frequency was assumed to be related to the shock wavefront velocity while the lower frequency was expected to be generated by the electromagnetic reflection on the metallic impactor or transfer plate. Assuming that the dielectric constant

of the shocked material is proportional to the mass density, Luther *et al.* derived from reflected electromagnetic waves the shock wavefront velocity and the refractive index of shocked materials. They indicated that the relationship between the permittivity and the mass density was not strictly valid. However, as the computation of a shock wavefront velocity is strongly dependent on the permittivity of the shocked material, any assumption on the dielectric constant may significantly limit the validity domain of the proposed model. Krall *et al.* ([*Krall et al.*(1993)] [*Sandusky et al.*(1993)]) developed an electromagnetic modeling for analyzing shocked porous materials in waveguides. The approach is based on the mass conservation at the shock wavefront and a mixture equation for the material permittivity. The shock wavefront and particle velocities in shocked melamine samples were derived from two specific oscillations observed in the reflected electromagnetic signal. According to Krall *et al.* ([*Krall et al.*(1993)]), the difference between the derived particle velocity and the velocity measured from streak camera does not exceed 7%. This method is valid for porous materials only and was applied to study a double-base ball propellant composed of nitroglycerin and nitrocellulose, the ionization of the shock front and the hot spot concentration ([*Sandusky et al.*(1993)]). Kanakov *et al.* ([*Kanakov et al.*(2008)]) studied the shock-compressed plastic fluor and were able to determine the shock wavefront velocity, the refractive index of the shocked material and the particle velocity. The electromagnetic model was applied to shocked material combining one static and two moving interfaces, but did not take into account the Doppler shift effect. Moreover seven parameters are needed for using the proposed model and consequently a complex and time-consuming optimization problem must be solved. The derived particle velocity agrees with the computation with a deviation of 2.7 %. Belskii *et al.* ([*Bel'skii et al.*(2011)]) developed an interesting method to analyze and interpret the double oscillation observed in the electromagnetic waves reflected by the shocked material. The method is based on the analysis of the ray propagation in a multi-layered material, involving the particle and shock wavefront velocities, and the relative permittivities of the unshocked and shocked materials ([*Bel'skii et al.*(2011)]). Numerical results were reported for various sets of parameters and the agreement with experimental data was found to be good. The results for benzene demonstrate that the method is accurate for the estimation of both velocities and allow determining the dielectric constant of the shocked material. However, a complex fitting technique using nine parameters is required for implementing the model.

In this paper, a new closed-form expression for the electromagnetic wave reflected by two moving interfaces is derived. The reflection of the incident linearly-polarized and time-harmonic electromagnetic field by interfaces moving at the same velocity has already been investigated for various incidences (see *e.g.* [*Yeh and Casey*(1965)]-[*Rad et al.*(1994)]) but the case of dielectric interfaces moving at different velocities is reported here for the

first time. As an application, the remote analysis of the shock wave phenomenon in solids is proposed. The main descriptors of shocked solids, *i.e.*, the shock wavefront velocity, the particle velocity and the refractive index behind the shock wavefront, are derived from measurable frequencies embedded in the reflected electromagnetic field. Physical insights on published measurement results are reported. New measurement data on shocked Poly-Methyl MethAcrylate (PMMA) are presented and discussed.

2 Electromagnetic Modeling

As sketched in Figure 1, we consider here two parallel and lossless interfaces moving at different constant velocities. The two velocities are $\vec{V_1} = V_1\vec{e}_z$ and $\vec{V_2} = V_2\vec{e}_z$, where $\vec{e}_z$ denotes the unit vector along the z axis. These velocities are very small compared with the speed of light in vacuum. At time $t = 0$, the two interfaces are located at $z = 0$, at time t, one interface is located at $z_1 = V_1 t$ and the other interface is located at $z_2 = V_2 t$. At any time t, it is assumed that $z_1 < z_2$. The separation distance between the two interfaces at time t is given by $|V_1 - V_2|t$. Moreover, we assume that both velocities are of the same sign. The interface 1 is dielectric while the interface 2 is a perfect electric conductor (infinite conductivity). Lossless dielectric material of (known) refractive index n_1 and (unknown) refractive index n_2 are placed on each side of interface 1. The linearly-polarized, transverse electric (TE) and time-harmonic field is normally incident on interface 1. This field is given by $\vec{\mathcal{E}}(z,t) = \vec{E}e^{j\omega t - jk_0 n_1 z}$, where ω denotes the radial operating frequency, $k_0 = \omega/c$ is the free-space wavenumber where c designates the speed of light in vacuum and E is the magnitude of the incident field. To obtain the electromagnetic field reflected by the two interfaces shown in Figure 1, we extend to moving interfaces the approach reported in ([*Ma and Okamura*(1999)]) for non moving (static) interfaces. The procedure is the following: at any time t, the separation distance between the two interfaces is given here by $|(V_1 - V_2)\,t|$ and the total reflected electric field $\vec{E_r}(z,t)$ combines two contributions. The first one, denoted $\vec{E_1}(z,t)$, results from the direct reflection of the incident field on the moving interface 1 and is given:

$$\text{for } z < V_1 t,\ \vec{E_1}(z,t) = \vec{E}R_{11}e^{j\omega_r t + jk_r z} \tag{1}$$

where R_{11} is the amplitude reflection coefficient given by by ([*Orfanidis*(2014)]):

$$R_{11} = \frac{1 - n_1\frac{V_1}{c}}{1 + n_1\frac{V_1}{c}} \times \frac{n_1 - n_2}{n_1 + n_2} \tag{2}$$

and where ω_r denotes the reflected radial frequency given as follows:

$$\omega_r = D_{R_{11}}\omega \tag{3}$$

with

$$D_{R11} = \frac{1 - n_1 \frac{V_1}{c}}{1 + n_1 \frac{V_1}{c}}. \tag{4}$$

In eq(1), k_r designates the wavenumber of the electromagnetic field reflected by the moving interface 1. From the Lorentz transformation ([*Orfanidis*(2014)]), the wavenumber k_r of the electromagnetic field reflected by the interface 1 is given as follows:

$$k_r = \frac{\omega}{c} \times \frac{n_1 - \beta}{1 + n_1 \beta} \tag{5}$$

where $\beta = V_1/c$ and $\gamma = 1/\sqrt{1-\beta^2}$.

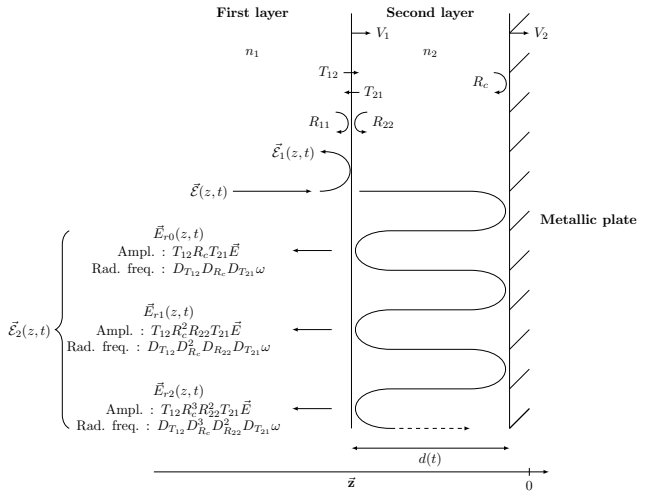

Figure 1: Configuration at time t with two moving interfaces: interface 1 (dielectric) and interface 2 (metallic) moving at constant velocities V_1 and V_2 respectively. At time $t = 0$, the two interfaces are located at $z = 0$ and consequently, the separation distance $d(t)$ between the two interfaces is given by $|V_1 - V_2|t$.

The second contribution, denoted by $\vec{E_2}(z,t)$, to the total reflected electric field, is derived from the electric field which is transmitted through interface 1. This field propagates from interface 1 to interface 2, is then reflected by interface 2 and next, propagates from interface 2 to interface 1 and is incident upon interface 1; the field transmitted through interface 1 contributes to the total reflected field while the field resulting from the reflection by interface 1 propagates from interface 1 to interface 2, is reflected by interface 2 and so on ... Multiple reflections take place between the two interfaces and as a consequence, the contribution $\vec{E_2}(z,t)$ to the total field reflected results in the sum of multiple contributions as follows:

$$\text{for } z < V_1 t,\ \vec{E}_2(z,t) = \sum_{p=0}^{\infty} \vec{A}_p e^{j\omega_p t + j k_r^{(p)} z} e^{j\varphi_p} \tag{6}$$

where

$$\vec{A}_p = \vec{E} T_{12} T_{21} R_c (R_c R_{22})^p \tag{7}$$

and

$$T_{12} = \frac{1 + n_2 \frac{V_1}{c}}{1 + n_1 \frac{V_1}{c}} \times \frac{2n_1}{n_1 + n_2} \tag{8}$$

$$R_{22} = \frac{1 + n_2 \frac{V_1}{c}}{1 - n_2 \frac{V_1}{c}} \times \frac{n_2 - n_1}{n_1 + n_2} \tag{9}$$

$$T_{21} = \frac{1 - n_1 \frac{V_1}{c}}{1 - n_2 \frac{V_1}{c}} \times \frac{2n_2}{n_1 + n_2} \tag{10}$$

$$R_c = \frac{1 - n_2 \frac{V_2}{c}}{1 + n_2 \frac{V_2}{c}} \times (-1) \tag{11}$$

and

$$\varphi_p = \frac{n_2 \omega}{c} D_{T_{12}} (1 + D_{R_c}) \sum_{i=0}^{i=p} (D_{R_c} D_{R_{22}})^i \tag{12}$$

In equation (6), ω_p denotes the radial frequency of the p-th contribution to $\vec{E}_2(z,t)$ and is given by (13) while p is the rank of the contribution to the electromagnetic field reflected by the moving interface 2.

$$\omega_p = D_{T_{12}} D_{T_{21}} D_{R_c} (D_{R_c} D_{R_{22}})^p \omega \tag{13}$$

where

$$D_{T_{12}} = \frac{1 + n_2 \frac{V_1}{c}}{1 + n_1 \frac{V_1}{c}} \tag{14}$$

$$D_{R_{22}} = \frac{1 + n_2 \frac{V_1}{c}}{1 - n_2 \frac{V_1}{c}} \tag{15}$$

$$D_{T_{21}} = \frac{1 - n_1 \frac{V_1}{c}}{1 - n_2 \frac{V_1}{c}} \tag{16}$$

$$D_{R_c} = \frac{1 - n_2 \frac{V_2}{c}}{1 + n_2 \frac{V_2}{c}} \tag{17}$$

The wavenumber $k_r^{(p)}$ in eq.(6) is derived from the transmission of the electromagnetic field at the p-th rank propagating along negative z direction and normally incident upon interface 1.From the Lorentz transformation ([*Orfanidis*(2014)]), the wavenumber $k_r^{(p)}$ can be written as follows:

$$k_r^{(p)} = \frac{\omega_p}{c} \times \frac{n_2 + \beta}{1 - \beta n_2}. \tag{18}$$

where ω_p is given in eq.(13).

From equations (1) and (6), the total electric field $\vec{E_r}(z,t)$ reflected by the two moving interfaces is then derived as follows:

$$\vec{E_r}(z,t) = \vec{E} R_{11} e^{j\omega_r t + jk_r z} + \sum_{p=0}^{\infty} \vec{A_p} e^{j\omega_p t + jk_r^{(p)} z} e^{j\varphi_p} \tag{19}$$

In order to ensure the numerical convergence of the series of eq.(6), $|R_c R_{22}|$ must be lower than 1. According to eq.(7) and eq.(11), this condition can be rewritten as follows:

$$\left| \frac{1 - n_2 \frac{V_2}{c}}{1 + n_2 \frac{V_2}{c}} \times \frac{1 + n_2 \frac{V_1}{c}}{1 - n_2 \frac{V_1}{c}} \times \frac{n_2 - n_1}{n_1 + n_2} \right| < 1. \tag{20}$$

As the velocities V_1 and V_2 are small compared with the velocity of light, eq.(20) can be expanded at first order as:

$$\left| 1 + 2\frac{n_2}{c} (V_1 - V_2) \times \frac{n_2 - n_1}{n_1 + n_2} \right| < 1. \tag{21}$$

Assuming $n_2 > n_1$, eq.(21) yields:

$$\left| 1 + 2\frac{n_2}{c} (V_1 - V_2) \right| < \frac{n_1 + n_2}{n_2 - n_1}. \tag{22}$$

As the velocities V_1 and V_2 are small compared with the velocity of light, the left term in eq.(22) is always positive. Therefore:

$$1 + 2\frac{n_2}{c} (V_1 - V_2) < \frac{n_1 + n_2}{n_2 - n_1}. \tag{23}$$

Finally, the condition for the convergence of eq.(6) is:

$$\frac{V_1 - V_2}{c} < \frac{n_1}{n_2(n_2 - n_1)}. \tag{24}$$

With V_1 and V_2 small compared with c and V_1 and V_2 of the same sign, this condition is true.

Moreover the velocities of the two interfaces are here small compared with the speed of light in vacuum. As a matter of fact, during a shock wave experiment in radio-transparent solids, the order of magnitude of $|V_1|$ and $|V_2|$ is respectively of $3000\,\mathrm{m\,s^{-1}}$ and $500\,\mathrm{m\,s^{-1}}$. Consequently, R_{11}, ω_r, A_p and ω_p given respectively by eqs (2), (3), (7) and (13) can be approximated as follows:

$$R_{11} \approx \frac{n_1 - n_2}{n_1 + n_2}\left(1 - 2n_1\frac{V_1}{c}\right) \tag{25}$$

$$\omega_r \approx \left(1 - 2n_1\frac{V_1}{c}\right)\omega \tag{26}$$

$$\left|\vec{A}_p\right| \approx \frac{4n_1n_2}{(n_1+n_2)^2}\left(1 + 2\frac{V_1}{c}(n_2 - n_1) - 2n_2\frac{V_2}{c}\right)\times\left(\frac{n_2 - n_1}{n_1 + n_2}\left(1 - 2n_2\frac{V_2}{c} + 2n_2\frac{V_1}{c}\right)\right)^p \tag{27}$$

$$\omega_p \approx \left(1 - 2n_1\frac{V_1}{c} - 2(p+1)n_2\frac{V_2 - V_1}{c}\right)\omega \tag{28}$$

Equations (26) and (28) can be rewritten using: $f_1' = |f_1 - f|$ and $f_p' = |f_p - f|$, with $f = \omega/2\pi$ as follows:

$$f_1' = |f_1 - f| = 2n_1\frac{V_1}{c}f \tag{29}$$

$$f_p' = |f_p - f| = \left(2n_1\frac{V_1}{c} + 2(p+1)n_2\frac{V_2 - V_1}{c}\right)f. \tag{30}$$

From eqs. (27), (29) and (30), the velocities V_1 and V_2 and the shocked refractive index n_2 can be written as a function of the measurable quantities $|A_1|$, $|A_2|$, n_1, f_1' and f_2'.

The frequency f_1' is associated with the reflection on the interface 1 while the frequency $f_2' = f_{p=0}'$ is associated with the field transmitted through the interface 1 and reflected by the interface 2. Let R_a be defined as the amplitude of the reflected field contribution of rank $p = 0$ normalized by the amplitude E of the incident field:

$$R_a = \frac{\left|\vec{A}_{p=0}\right|}{R_{11}} \tag{31}$$

The refractive index n_2 of the shocked material is solution of:

$$R_a n_1^2 + 4n_1n_2\left(1 - \frac{f_1' - f_2'}{f}\right) - R_a n_2^2 = 0. \tag{32}$$

where the refractive index n_1 of the host material is known. The discriminant $\triangle$ of this quadratic polynomial is:

$$\triangle = 16n_1^2\left(1 - \frac{f_1' - f_2'}{f}\right)^2 + 4n_1^2R_a^2 \tag{33}$$

Since this discriminant is positive, eq (32) has two real-valued solutions for n_2, given by:

$$n_2 = \frac{-4n_1\left(1 - \frac{f_1' - f_2'}{f}\right) \pm \sqrt{\triangle}}{2R_a} \tag{34}$$

Parameter	Value
Operating frequency	9 GHz
Frequency f_1'	56 kHz
Frequency f_2'	5.6 kHz
Shock velocity V_1	$558\,\mathrm{m\,s^{-1}}$
Particle velocity V_2	$164\,\mathrm{m\,s^{-1}}$
Unshocked relative permittivity ε_1	2.86
Shocked relative permittivity ε_2	3.86
Measurement time	179 ms

Table 1: Values given in [*Krall et al.*(1993)] for shocked melamine

According to eqs. (29) and (30), as the velocities $|V_1|$ and $|V_2|$ are small compared with the velocity of light c, the frequencies f_1' and f_2' are much smaller than the operating frequency f and consequently, it can be easily demonstrated that only the following solution is positive and then acceptable:

$$n_2 = \frac{-4n_1\left(1-\frac{f_1'-f_2'}{f}\right)+\sqrt{\triangle}}{2R_a} \tag{35}$$

Moreover, from eqs. (29) and (30), the velocities V_1 and V_2 can be derived as follows:

$$V_1 = \frac{c}{2n_1}\frac{f_1'}{f} \tag{36}$$

$$V_2 = V_1 + \frac{c}{2n_2}\frac{f_2'-f_1'}{f}. \tag{37}$$

Based on eqs.(35), (36) and (37), the velocities V_1 and V_2 can be derived from the measurable quantities R_a, n_1, f_1' and f_2'.

3 Results and Discussion

3.1 Application to shocked melamine material

To test the validity of the proposed model, the results are compared with reported data on melamine ([*Krall et al.*(1993)]). First, we use our model to compute the frequencies f_1' and f_2' with the published values for velocities and refractive index reported in Table 1. The amplitude ratio is found to be of 10. The relative deviation from published data is reported in Table 1. The shock wavefront velocity is successfully computed and the particle velocity is in the same order of magnitude.

	V_1 ($\mathrm{m\,s^{-1}}$)	V_2 ($\mathrm{m\,s^{-1}}$)	n_2
Published data	558	164	1.96
This work	552 ± 57	145 ± 59	2.06 ± 0.031
Deviation (%)	1.1%	11.6%	4.9%

Table 2: Comparison between the data reported in [*Krall et al.*(1993)] and the computed values of velocities and shocked refractive index for $f_2' = 5.6\,\mathrm{kHz}$ and $f_1' = 56\,\mathrm{kHz}$

Parameter	Value	Fitting error
f_1'	3.30 MHz	103 kHz
f_2'	313 kHz	3.69 kHz
R_a	28.8	3.7

Table 3: Fitted parameters for the impact of an iron disc on a PMMA target at $510\,\mathrm{m\,s^{-1}}$

3.2 Application to shocked PolyMethyl MethAcrylate material

As a second benchmark case, the propagation of a shock wave in a PolyMethyl MethAcrylate material (PMMA) material is studied. A plane impact on a PMMA target (thickness of 15 mm) is generated with a light gas gun at a velocity of $510\,\mathrm{m\,s^{-1}}$. The impactor is an iron (Fe α) disc of 11 mm in thickness and of 30 mm in diameter. A continuous electromagnetic field with an operating frequency of 94 GHz is transmitted into the target. The measured reflected signal is shown in fig 2. After the impact, at t$\approx$372 µs, two oscillations are observed in the signal. To estimate the input parameters for the model, a fit of the form of eq. (38) is performed.

$$S(t) = A_1 \sin(2\pi f t + \varphi_1) + A_2 \sin(2\pi f t + \varphi_2) \tag{38}$$

The results are given in Table 3. The model is then applied, and the velocities and the refractive index of the media under shock loading are listed in Table 4. Compared to the melamine case, the uncertainties here are lower, due to the higher operating frequency. With a Mie-Gruneisen equation of state for the iron ([*Brown and Ravichandran*(2014)]) and the PMMA ([*Marsh*(1980)]), the impedance matching method yields $V_1 = 3147\,\mathrm{m\,s^{-1}}$ and $V_2 = 463\,\mathrm{m\,s^{-1}}$. The result from hydrodynamic methods and the proposed measurement technique are in good agreement.

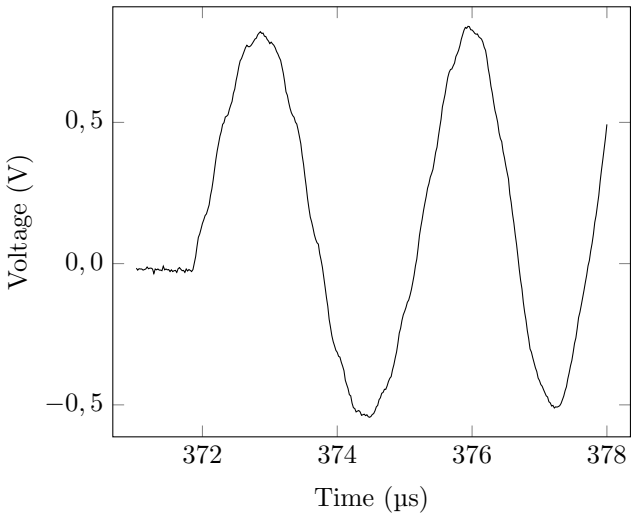

Figure 2: Reflected signal for the impact of an iron disc on a PMMA target at $510\,\mathrm{m\,s^{-1}}$.

Parameter	Value	Uncertainty
V_1	$3141\,\mathrm{m\,s^{-1}}$	$113\,\mathrm{m\,s^{-1}}$
V_2	$489\,\mathrm{m\,s^{-1}}$	$32\,\mathrm{m\,s^{-1}}$
n_2	1.79	0.016

Table 4: Velocities and refractive index of the shock loaded PMMA.

4 Conclusion

This paper describes a closed-form expression reports the electromagnetic field reflected by two moving interfaces. Doppler frequency shifts and relativistic effects are here explicitly developed. This model can be derived into a first order developed expression that gives estimation of the interface velocities and the refractive index of the shocked material. Applications to the data published on shocked melamine and to new experimental results on shocked PMMA are reported. The results from hydrodynamic methods and the proposed measurement technique are in good agreement. The electromagnetic modeling of shocked material by taking into account eventual multiple moving interfaces behind the shock wavefront is under progress in our research team. Dedicated experiments, where the estimated particle velocity could be compared with measurement data, will be performed in order to test the validity domain of the proposed modeling.

The authors wish to thank Thomas Chazoule for his contribution to this work. They acknowledge CEA/DAM Gramat (France) and the Occitanie Regional Council (France) for financial support. Besides, the authors would like to thank colleagues from CEA for appreciation and helpful advices on

different topics. The authors would like to thank the anonymous reviewer for his assistance in evaluating this paper. All data used is available in the listed references or in the supporting data online.

References

[*Meyers*(1994)] Meyers, M. A. (1994)., Dynamic Behavior of Materials. *John Wiley and Sons.*

[*Cox and Merz*(1958)] Cox, W.P. and Merz, E.H. (1958). The density dependance of the dielectric constant of polyethylene. *Journal of polymer science.* 28, 622–625.

[*Anderson and Kelly*(1967)] Anderson, G. A. and Kelly, J. G (1967). Continuous Measurement of Shock and Contact Discontinuities Velocity. *IEEE AES* 3, 613–622.

[*Koch*(1969)] Koch, B. (1969). Digital Measurement of the Speed Variations of Shock Waves by Means of Microwaves. *Physics of Fluids.* 12, I-144–I-146.

[*Luther et al.*(1991)] Luther, G. G., Veeser, L. and Warthen, B. J. (1991). A Microwave Interferometer to Measure Particle and Shock Velocities Simultaneously. Shock Compression of Condensed Matter, *Elsevier Science Publishers B.V.*.

[*Luther and Warren*(1994)] Luther, G. G. and Warthen, B. J. (1994). Microwave interferometry to elucidate shock properties, *AIP Conference Proceedings.* 309, 1755–1757.

[*Marsh*(1980)] Marsh, S. P. (1980). LASL Shock Hugoniot Data, *University of California Press.*

[*Krall et al.*(1993)] Krall, A. D., Glancy, B. C. and Sandusky, H. W. (1993). Microwave interferometry of shock waves. I. Unreacting porous media. *J. Appl. Phys.*. 74, 6322–6327.

[*Sandusky et al.*(1993)] Sandusky, H. W., Glancy, B. C. and Krall, A. D., (1993). Microwave interferometry of shock waves. II. Reacting porous media. *J. Appl. Phys.*. 74, 6328–6334.

[*Kanakov et al.*(2008)] Kanakov, V. A., Lupov, S. Yu., Orekhov, Yu I and Rodionov, A. V. (2008). Techniques for retrieval of the boundary displacement data in gas-dynamic experiments using millimeter-waveband radio interferometers. *Radiophysics and Quantum Electronics.* 51, 210–221.

[*Bel'skii et al.*(2011)] Bel'skii, V. M., Mikhailov, A. L., Rodionov, A. V. and Sedov, A. A. (2011). Microwave Diagnostics of Shock-Wave and Detonation Processes. *Combustion, Explosion and Shock Waves*. 47, 639–650.

[*Yeh and Casey*(1965)] Yeh, C. and Casey, K.F. (1966). Reflection and Transmission of Electromagnetic Waves by a Moving Dielectric Slab. *Phys. Rev.*. 144, 665.

[*Wang and Zhang*(2010)] Wang, H. and Zhang, X. (2010). Magnetic response induced by a moving dielectric slab. *J. Appl. Phys*. 107, 104108.

[*Rad et al.*(1994)] Rad, A., Abdolali, A. and Salary, M. M. (2014). Interaction of Electromagnetic Waves with a Moving Slab: Fundamental Dyadic Method. *PIER B*. 60, 1–13.

[*Orfanidis*(2014)] Orfanidis, S. J. (2014). Electromagnetic Waves and Antennas. *Rutgers University*.

[*Ma and Okamura*(1999)] Ma, Z. and Okamura, S. (1999). Permittivity Determination Using Amplitudes of Transmission and Reflection Coefficients at Microwave Frequency. *IEEE Transactions on Microwave Theory and Techniques*. 47, 546–550.

[*Brown and Ravichandran*(2014)] Brown, J.L. and Ravichandran, G. (2014). Analysis of oblique shock waves in solids using shock polars. *Shock waves*. 24, 403–413.

[*GUM*(2008)] GUM (2008). Evaluation of measurement data - Guide to the expression of uncertainty in measurement. *JCGM*.